CSIRO Publishing

Publications of the Astronomical Society of Australia

VOLUME 18, 2001

An international journal of astronomy and astrophysics

For editorial enquiries and manuscripts, please contact:
The Editor, PASA,
ATNF, CSIRO,
PO Box 76,
Epping, NSW 1710, Australia
Telephone: +61 2 9372 4590
Fax: +61 2 9372 4310
Email: Michelle.Storey@atnf.csiro.au

For general enquiries and subscriptions, please contact:
CSIRO Publishing
PO Box 1139 (150 Oxford St)
Collingwood, Vic. 3066, Australia
Telephone: +61 3 9662 7666
Fax: +61 3 9662 7555
Email: pasa@publish.csiro.au

Published by CSIRO Publishing
for the Astronomical Society of Australia

www.publish.csiro.au/journals/pasa

Publ. Astron. Soc. Aust., 2001, 18, 329–335

Generation of Coronal Currents by the Solar Convection Zone

D. J. Galloway[1], Y. Uchida[2] and N. O. Weiss[3]

[1]School of Mathematics and Statistics, University of Sydney,
NSW 2006, Australia
[2]Department of Physics, Science University of Tokyo, Kagurazaka,
Shinjuku-ku, 162 Tokyo, Japan
[3]Department of Applied Mathematics & Theoretical Physics, University of Cambridge,
Cambridge CB3 9EW, UK

Received 2001 September 7, accepted 2001 September 20

Abstract: Solar flares are thought to be caused by reconnection of magnetic fields and their associated electric currents in the solar corona. The currents have to be there to provide available energy over and above the current-free minimum energy state, but what generates them has been little discussed. This paper investigates the idea that twisting motions in the turbulent convection zone below may provide a natural source for the currents and explain some of their properties. The twists generate upward-propagating Alfvén waves with a Poynting flux of the right order of magnitude to power a flare. Depending on the depth it takes place, the twisting event that initiates a particular flare may occur hours, days or even months before the flare itself.

Keywords: Sun: magnetic fields — convection — MHD — Sun: corona — Sun: flares

1 Introduction

The Sun's magnetically dominated atmosphere is constantly changing as it is subjected to a large variety of disturbances initiated by events taking place at the photosphere and deeper down. If left to itself, the coronal magnetic field **B** would eventually relax to its minimum energy state, that of a potential field with no electric currents. The associated magnetic structure is then found by solving Laplace's equation with an assumed distribution of the normal component of **B** at the photosphere, the latter usually inferred from observations (Schmidt 1964, and numerous later authors). Models constructed in this way reproduce the crude features of the coronal magnetic field, but to explain phenomena that involve energy release, such as flares, there have to be currents that raise the energy above its minimum level.

Observational attempts to determine the currents flowing into the corona use vector magnetographs to measure the horizontal field components B_x and B_y using spectral lines formed at photospheric levels. The vertical component of the total current inside any region can then be inferred from Ampère's Law, or (more dangerously, if the data is noisy) numerical differentiation can be used to estimate the vertical component of the curl, and hence the current density. On this basis, it has been claimed that active region magnetic flux concentrations sometimes carry currents up to the order of several times 10^{12} A. Furthermore, these currents are frequently 'unbalanced', i.e. no corresponding return currents are observed inside or immediately adjacent to the relevant flux concentration (see Pevtsov, Canfield, & Metcalf 1994; Leka et al. 1996). A recent discussion of this, with more references, is given in Longcope et al. (1999), where an attempt is made to identify the origin of the twists. Several possibilities are examined, and the conclusion is that the twisting is due to the buffeting of flux tubes by eddies in the solar convection zone. These have helicity and so impart twist.

The existence of unreturned vertical currents is exploited in a theory for solar flares put forward by Melrose (1995, 1997). In this, the reconnection of magnetic fields present in many other theories is accompanied by a reconnection of currents (see Figure 1). Before and after the flare the same unbalanced currents emerge from or enter the same flux concentrations, but their paths through the corona change to connect different concentrations. A simple circuit model is used to show that the associated change in inductive energy is easily sufficient to power the flare. There has been criticism of this model by Parker (1996; see also the accompanying reply by Melrose 1996). The most important point is whether the observations indeed pin down the absence of return currents, or whether they are really there but are concealed by noise and lack of resolution. This is a very important question but until it is observationally settled theoreticians should be allowed to keep an open mind.

This paper describes a numerical model which demonstrates how convective twisting events located somewhere in the convection zone can supply the corona with a Poynting flux possessing sufficient energy to power flares. It also goes some way to explaining how, within the confines of the axisymmetric geometry adopted, return currents may be expected to occur not adjacent to the flux tube being twisted, but some distance away. Its purpose is not to justify the Melrose model — this requires an MHD calculation in circumstances appropriate to the corona — but to explain how the prerequisites for the model may be supplied by what is happening deep within the convection zone.

 10.1071/AS01057 1323-3580/01/04329$05.00

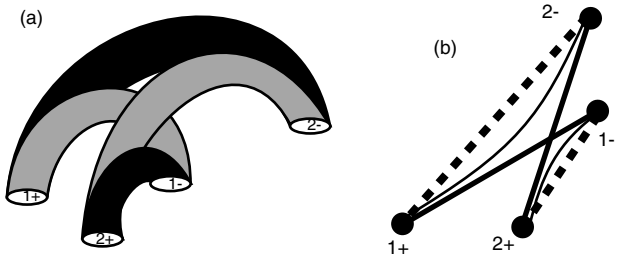

Figure 1 A schematic diagram of the Melrose (1997) model for loop flares. On the left, (a) shows initial loops 1 and 2 (lightly shaded) connecting footpoints 1+, 1−, and 2+, 2−, respectively, before reconnection. After reconnection, loops 3 and 4 (shaded dark) connect footpoints 1+, 2−, and 2+, 1−, respectively. On the right, (b) shows how the loops reconnect when viewed from above, with heavy solid lines denoting initial loops, heavy dashed lines denoting final loops, and light lines indicating field/current lines in the process of transferring from the initial to the final loops.

Details of the model are given in Section 2, which describes a calculation where axisymmetric Boussinesq magnetoconvection is allowed to develop an axial flux tube which is subsequently twisted by rotating the outer periphery. Results and their interpretation are given in Section 3, and Section 4 concludes by discussing the implications for the Sun, the limitations and possible extensions of the model, and the implications for the Melrose theory of flares.

2 Description of the Computations

The equations solved are those of Boussinesq magnetoconvection: the Navier–Stokes equation with back-reaction of the Lorentz force, the induction equation, the equation for heat conduction in a moving medium, the incompressibilty condition and equation of state for a Boussinesq fluid, and the MHD approximation for the current. The reader is referred to Jones & Galloway (1993) for a listing of these; in a moment we will give the scaled versions used in the actual computations. In an axisymmetric geometry, this set divides into three evolution equations for the meridional variables and two for the twist ones. In cylindrical polar coordinates (r, ϕ, z), the solenoidality conditions for velocity $\mathbf{u}$ and magnetic field $\mathbf{B}$ allow the definition of stream and flux functions ψ and χ such that

$$\mathbf{u} = \nabla \times \left(-\frac{1}{r}\frac{\partial \psi}{\partial z}, u_\phi, \frac{1}{r}\frac{\partial \psi}{\partial r} \right),$$

$$\mathbf{B} = \nabla \times \left(-\frac{1}{r}\frac{\partial \chi}{\partial z}, B_\phi, \frac{1}{r}\frac{\partial \chi}{\partial r} \right).$$

The curves $\psi = \text{constant}$ and $\chi = \text{constant}$ give the streamlines of the meridional flow and the field lines of the poloidal magnetic field respectively. The natural variables to use for a numerical solution are those that are conserved under advection by the convective flow. These are the potential vorticity $\Omega = (\nabla \times \mathbf{u})_\phi / r$, the magnetic flux function χ defined above, the temperature T, the specific angular momentum $h = r^2\omega$, and the quantity $b \equiv B_\phi / r$. When the equations are scaled in units of the height of the cylinder, the thermal diffusion time, the input mean vertical magnetic field B_0, and the temperature difference ΔT between the top and bottom boundaries, the following set results:

$$\frac{\partial \Omega}{\partial t} + \nabla \cdot (\Omega \mathbf{u}) = \nabla \cdot \left(\frac{h^2}{r^4}\hat{\mathbf{z}} \right) + \frac{Q\sigma}{q} \nabla \cdot (\mathbf{B}J - b^2\hat{\mathbf{z}}) - R\sigma \nabla \cdot \left(\frac{\hat{\mathbf{r}}T}{r} \right) + \sigma \nabla \cdot \left(\frac{1}{r^2} \nabla (r^2 \Omega) \right)$$

$$\frac{\partial \chi}{\partial t} + \nabla \cdot (\chi \mathbf{u}) = \frac{1}{q} \nabla \cdot \left[r^2 \nabla \frac{\chi}{r^2} \right]$$

$$\frac{\partial T}{\partial t} + \nabla \cdot (T\mathbf{u}) = \nabla^2 T$$

$$\frac{\partial h}{\partial t} + \nabla \cdot (h\mathbf{u}) = \frac{Q\sigma}{q} \nabla \cdot (\mathbf{B} r^2 b) + \sigma \nabla \cdot \left[r^2 \nabla \frac{h}{r^2} \right]$$

$$\frac{\partial b}{\partial t} + \nabla \cdot (b\mathbf{u}) = \nabla \cdot \left(\mathbf{B}\frac{h}{r^2} \right) + \frac{1}{q} \nabla \cdot \left(\frac{1}{r^2} \nabla (r^2 b) \right).$$

In addition it is necessary to solve a Poisson equation $\nabla \cdot ([\nabla \psi]/r^2) = -\Omega$ in order to determine the stream function at each timestep, and to evaluate the variable $J = -\nabla \cdot ([\nabla \chi]/r^2)$ which is the ϕ-component of the current divided by r. The non-dimensional numbers here are the Rayleigh number R, proportional to the imposed temperature gradient, the Chandrasekhar number Q, proportional to the square of the imposed mean vertical magnetic field, and the Prandtl and Roberts numbers $\sigma = \nu/\kappa$ and $q = \kappa/\eta$, which are diffusivity ratios. An additional parameter is the ratio of cell radius to height, which is set to unity in these computations. The notation here is fairly standard, but see Jones & Galloway (1993) for full definitions of all quantities.

These equations have been given at length because they show clearly which quantities are conserved in the absence of diffusion and back reactions of any forces on the right hand side. Over much of the flow domain, away from certain key locations, these RHS terms are small and the figures in the next section can largely be understood by thinking in terms of these conserved quantities, particularly χ, h, and b.

As well as the equations, we must consider the boundary conditions. These are crucial and need to be selected very carefully to model twisting as it might happen in the solar convection zone. The frames in the results plotted in Figure 2 show the process we have in mind. A flux tube extending vertically through the convection zone is subjected to a twisting event by a region where there is a local preferred sense of rotation (since in reality the convection is turbulent, this will inevitably happen from time to time, even disregarding the overall solar rotation). In regions where the flow converges towards the tube axis, angular momentum from the body of the convection cells above and below will be swept inwards, spinning up in the process. The resulting differential rotation will twist the tube up, resulting in the generation of torsional Alfvén waves which propagate upward and downward from the location

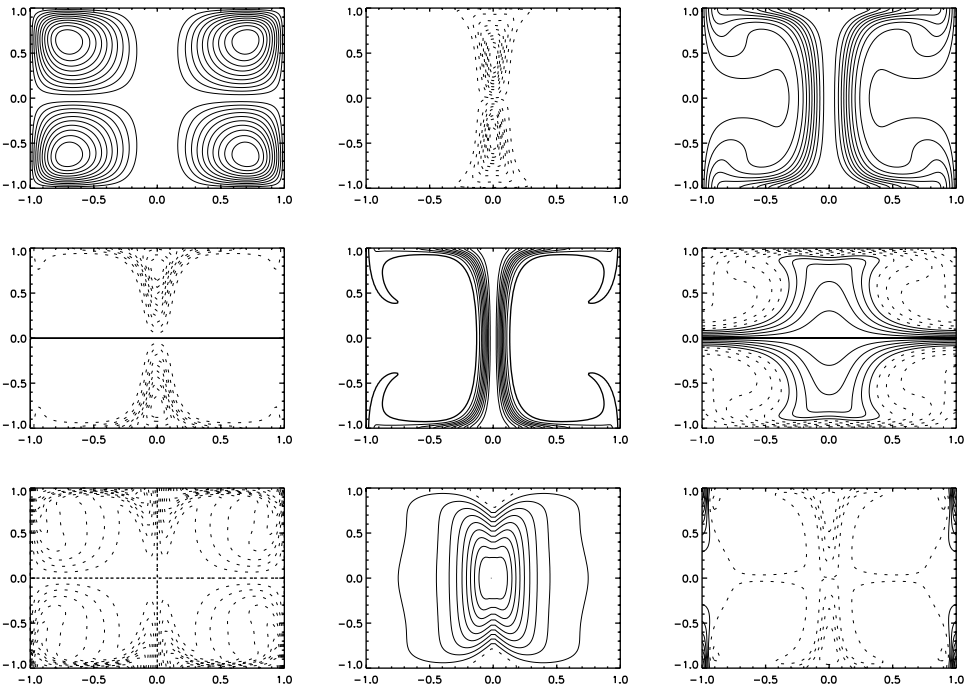

Figure 2 Computed and derived fields for the steady state solution described in the text. The basic twisting site is in the centre of each frame; the axis runs vertically through the centre and there are two toroidal eddies in the top and bottom halves of the cell, shown in cross-section. These eddies converge towards the axis at the centre. The time has reached 1.02 in units of the thermal diffusion time. Represented in the 9 frames are, scanning from top left to bottom right: the meridional stream function ψ, the potential vorticity Ω, the specific angular momentum h, the azimuthal field variable $b = B_\phi / r$, the meridional flux function χ, the temperature T, B_ϕ itself, ω itself, and the vertical component of the current j_z. See text for further details.

of the twisting site. Depending on the persistence of the anomalous rotation, this will take place either as a transient or, if the rotation continues unabated, it eventually evolves to a steady state. In either case energy is passed away from the twisting site as a Poynting flux, upwards at the top boundary and downwards at the bottom.

In Figure 2, the upper and lower cells are mirror images of one another as long as the fluid is Boussinesq, and we actually only solve in the top one. At the latter's lower boundary $z = 0$, B_ϕ is changing from one sign to the other and the rotation rate is locally a maximum, so appropriate boundary conditions are that b and $\partial h/\partial z$ are zero there. At the top boundary waves will pass out of the domain, so it is appropriate to take $\partial b/\partial z$ and $\partial h/\partial z$ zero there. At the outer periphery we take $b = 0$. By Ampère's Law this means there is no net vertical current through the layer. In view of our stated aim to investigate whether unbalanced currents are possible this might seem perverse, but in fact any other choice predetermines the issue, and more is learned by forcing the return currents to be there and then observing precisely where they are located.

An untwisted tube is first formed by allowing a non-rotating convection cell to focus an initially uniform vertical magnetic field into a steady concentration surrounding the axis. Twisting is then initiated by rotating the outer boundary at a uniform rate. Viscosity transfers this rotation to the interior of the cell, where it is swept towards the axis and spun up by the meridional circulation.

The remaining boundary conditions on the non-twist quantities are less critical and are fully described in Jones & Galloway (1993). The equations were solved numerically by the finite-difference scheme described in an appendix to that paper.

3 Results

The calculation to be described takes values $R = 10\,000$, $Q = 5$, $\sigma = 1$, $q = 5$, (cell radius)/height $= 1$, and a specific angular momentum $h_0 = 1$ imposed at the outer periphery for $t > 0.35$ diffusion time units, after the untwisted flux tube has evolved to a steady state. These values are many orders of magnitude less extreme than those prevailing in the solar convection zone, but should nonetheless be representative of the physics we wish to include (it is numerically quite impossible to compute solutions for the true solar values). R is taken large enough to ensure vigorous convection, and the chosen Q gives a magnetic field weak enough to allow effective convection but strong enough to be dynamically active when concentrated into a flux rope. The value taken for σ gives a viscosity small enough to allow approximate conservation of angular momentum but large enough to transmit the applied rotation into the body of the cell. The fluid needs to be a good electrical conductor to form a flux tube at all, and this is achieved by taking a high value for q. We expect that since our subsequent results depend more on the the effects of advection than diffusion, the same basic phenomena will take place on the Sun. Even though the

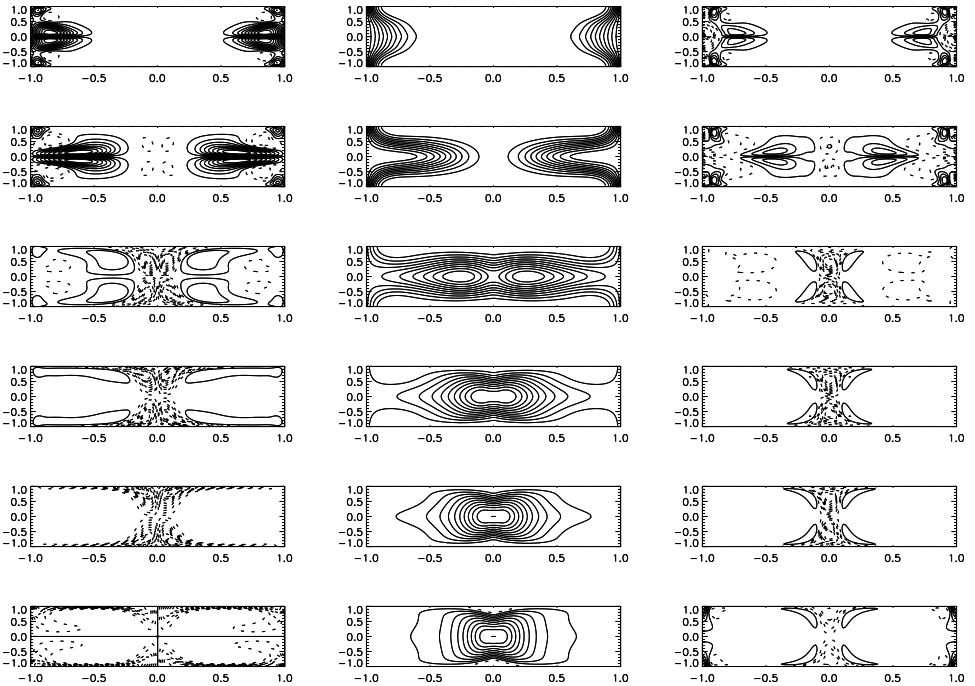

Figure 3 Evolution of the twist field B_ϕ, the angular velocity ω, and the vertical current density j_z, during the transient phase. The rotation of the outer cylinder wall is turned on at $t = 0.35$, and successive rows are at times 0.358, 0.368, 0.377, 0.387, 0.397, and 0.425. (By this last time the return currents at the outer periphery are established.) The time unit is again the thermal diffusion timescale. The cells are squashed to fit on the page.

laminar diffusivities are many orders of magnitude lower there, turbulence effectively raises them again, albeit to a currently unquantifiable extent.

As soon as the rotation has been advected into the central flux tube it starts to generate torsional Alfvén waves and there is a transient phase. This takes place very quickly because the Alfvén speed is locally high within the tube. Thereafter, there is a gradual evolution to a steady state. Figure 2 illustrates this eventual steady state, giving plots of the meridional stream function ψ, the five advected fields Ω, χ, T, h, and b, and the associated B_ϕ, rotation rate ω, and vertical component of current density j_z. Figure 3 gives the time evolution of the transient, plotting only the twist-associated quantities B_ϕ, ω, and j_z (the evolution of the other quantities is less interesting).

To examine the propagation of twist energy into the region above the convecting layer, it is instructive to calculate the upward directed Poynting flux $(\mathbf{E} \times \mathbf{B})_z/\mu_0$ per unit area at the top boundary. Using Ohm's law for the electric field $\mathbf{E}$, this can be shown to be equal to $-(r\omega B_\phi B_z)/\mu_0$. For the present calculation, we have imposed positive rotation rate and mean magnetic field, and this means the flux is upward if B_ϕ and B_z have opposite signs at the top. Figure 4 gives plots of these two quantities with r, showing that apart from the initial instant of the transient, this is indeed the case. This generation of negative B_ϕ is straightforward to understand in terms of the differential rotation that is set up. Other choices of sign for the rotation rate and mean field give the same result for the sense of the Poynting flux; the only crucial thing is that the meridional convective circulation has the sense indicated.

The plots showing the evolution of j_z illustrate where the return currents accumulate. Except right at the start of the transient, these are found predominantly at the outer periphery of the cell, and not surrounding the axial flux tube. A similar result was found in Galloway & Jones (1995) for a calculation done in a different context. The reason for this effect can be understood by observing that away from boundary layers the quantity $b = B_\phi/r$ is approximately conserved. This means that as b is towed across from the axis to the periphery just under the top boundary, B_ϕ scales as r. The vertical current density j_z is proportional to $(1/r)\partial(rB_\phi)/\partial r$ and thus scales as a constant. This explains why the contours of j_z are almost horizontal just under the top boundary away from the flux rope and the periphery. As r increases from zero, j_z is large and negative near the axis, then terraces for the reason just described, and finally becomes large and positive near the periphery in order to meet the condition that there is no net total current through the layer, as required by the $B_\phi = 0$ outer boundary condition. The return current, here positive, is thus generated at the outer boundary of the cell.

The version of this problem with no twists was investigated much earlier, numerically by Galloway & Moore (1979), and analytically by Galloway, Proctor, & Weiss (1978), and Proctor & Galloway (1979). The addition of twists makes little difference to the structure of the meridional variables. The strength of B_ϕ depends on the rate at which the outer boundary is rotated. We have chosen a

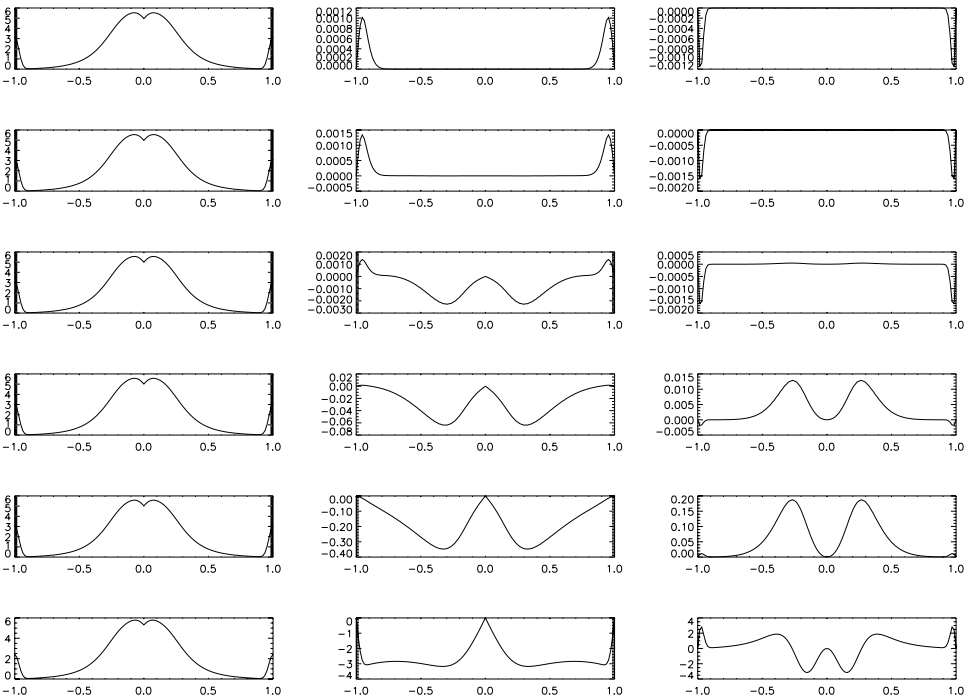

Figure 4 Evolution of the field components B_r (left) and B_ϕ (right), plotted as a function of r across the top of the cell (going across a whole diameter), during the transient phase and in the steady state. The rotation of the outer cylinder wall is turned on at $t = 0.35$; successive rows are at times 0.358, 0.368, 0.378, 0.387, 0.397, and 1.02 (the steady state). The time unit is the thermal diffusion timescale. The small region of negative Poynting flux surrounding the axis in the last frame is due to the existence of a slow retrograde rotation in this region.

rate that gives B_ϕ of the same order as B_z in the flux tube (cf. Figure 4), though we also did other runs where it was an order of magnitude larger. In the fully three-dimensional case, these would be subject to a variety of instabilities (as, in practice, would the untwisted case). Since twists of order one are thought to aid in stabilisation, we have presented such a case here.

4 Discussion

The calculation in the last section achieves two important goals. First, it demonstrates a clear mechanism whereby turbulent convection can generate torsional Alfvén waves which carry a significant Poynting flux away from the twisting site. Second, it gives a reason why the corresponding return currents may arise some distance away from the outgoing currents associated with the twisting of the flux tube itself. Reconnection of horizontal fields at the edges of adjacent convection cells may cause the balance of current to take place even further away in a full non-axisymmetric convection pattern. This gives a justification for the locally unbalanced current configurations used in the Melrose (1995, 1997) theory for solar flares.

The twisting mechanism investigated here is related to but distinct from the 'Σ-effect' proposed by Longcope, Fisher, & Pevtsov (1998). In that paper, convective turbulence is again advanced as a likely source of the observed twist, but the thin flux tube approximation is used, and the effect of the convection is to cause buckling and coiling of the tube axis. Such an effect does not appear in any axisymmetric model, and is complementary to the work presented here.

The actual Poynting flux involved is substantial. An estimate based on supergranules and sunspot-type field strengths for B_r and B_ϕ gives a figure of the order of 10^7 W m^{-2}. This is far more than is needed to heat the solar corona (Priest 1982), though this figure is likely to be reduced because the Poynting flux only comes through a fraction of the top of the cell, and much of the energy production may be in the form of transients. The question then becomes where this energy goes, in particular whether it is reabsorbed on its journey up through the convection zone, or whether it enters the corona and goes right through it.

To resolve these issues requires a more detailed model than that presented here. We have used an axisymmetric geometry with no underlying background stratification, without any overlying coronal model to predict the fate of the waves once they arrive there. Some comments about reabsorption are possible if circumstances permit a WKB approach where the wavelength is small compared to the scale height. Then, to lowest order, there is no reabsorption and the waves propagate out at the local Alfvén speed. If we assume that deep down field strengths correspond to convective equipartition (Galloway, Proctor, & Weiss 1977), this means the transit time for the waves is of the order of the convective turnover time. This is around a day for disturbances initiated by supergranules, and of order a month for disturbances generated in the lower half of

the convection zone. Thin flux tube modellers believe the actual field strengths need to be up to 10 times higher than this to explain flux emergence characteristics at the photosphere (D'Silva & Choudhuri 1993; see other papers cited in Longcope et al. 1999). In that case these times would be up to ten times less, but they are still long — if deep twisting events send up disturbances which trigger solar flares, the event responsible for a particular flare may have taken place long before. This conclusion is unlikely to change significantly in the non-WKB case. However, the WKB prediction regarding reabsorption is likely to be very unreliable, particularly in view of the turbulence present throughout the convection zone. Note that Uchida et al. (in preparation) have performed preliminary axisymmetric calculations in a compressible fluid to assess the degree of reflection at a transition from high- to low-β region. (Here the plasma β is the ratio of gas pressure to magnetic pressure.) The wave is initially reflected but subsequently modifies the boundary and finally emerges as a nonlinear 'bullet'.

If the waves do get through, what happens to them in the corona? Alfvén waves are notoriously difficult to absorb there, and the most likely outcome is that those on open field lines propagate out into the solar wind, whilst those on loops return to the photosphere. In the latter case, it is not even clear how the corona can sustain anything *other* than transient twists (cf. Wheatland & Melrose 1994) — perhaps such waves are perpetually present as transients in the corona but have a non-obvious observational signature. Occasionally they may trigger flares by acting as 'the straw that breaks the camel's back' in pushing a coronal magnetic field configuration into a catastrophe where a possible equilibrium suddenly ceases to exist. The loop flare model of Uchida & Shibata (1988) shows a numerical calculation where torsional waves released simultaneously at the loop footpoints collide at the loop apex and provoke just such a catastrophe; see also Miyagoshi et al. (2001), and Uchida et al. (2001). Wheatland & Uchida (1999) have analysed statistics of transient loop brightenings versus loop flares to show that the relative frequencies are consistent with a picture where one wave on its own causes a brightening whilst two colliding waves provoke a flare.

Concerning whether a twisting event has enough energy to be responsible for a loop flare, there are two cases to consider. If the magnetic configuration is prestressed and the twisting event merely acts as a trigger, a relatively small Poynting flux suffices in addition to what was already stored in the non-potential field. However, the twist can also have enough energy to do the job on its own. This is what happens in the Uchida & Shibata (1988) model. A Poynting flux of 10^7 W m^{-2} over an area with radius 10 000 km lasting 1 h gives a total energy of order 10^{25} J, sufficient for even the largest flares, though these are usually two-ribbon rather than loop flares.

A natural question is whether there is any way to observe propagating twists in the corona. One certainly sees visual evidence of twists in images of some features, such as the famous 'Grandaddy' eruptive prominence of 1946 (see e.g. Priest & Forbes 2000, p. 4). However, the observations are usually over too long a timescale, or are repeated too infrequently, to be able to say much about the detailed time dependence. Data from TRACE so far have the highest cadence rate, and our hope is that this paper will inspire a careful search. Higher time resolution of variations in the horizontal components of photospheric magnetic fields would also be worthwhile. This could perhaps be done near the solar limb by using a magnetograph to measure the field in the undisturbed photosphere just outside a sunspot. Ampère's law demands twist fields there of several hundred gauss if there are to be unbalanced currents of several times 10^{12} A coming out of the spot. Northward and southward of the spot these would have opposite signs, and variations on timescales of minutes to hours would be detectable (though they might only be present a fraction of the time).

This paper has only examined the generation of torsional Alfvén waves; treating other wave modes is harder because it requires the addition of compressibility and non-axisymmetry. In reality all modes will be present on the Sun, and a full calculation which establishes their relative importance and superposes a corona into which the various waves can propagate remains a formidable challenge.

Acknowledgments

We are grateful to the Japan Society for the Promotion of Science and the Australian Research Council for funding travel which permitted two authors to visit the third at the Science University of Tokyo. The code used was developed in collaboration with Dan Moore and Chris Jones. DJG would also like to thank Don Melrose for providing Figure 1, and for numerous enthusiastic and inspiring conversations during our years together at the University of Sydney.

References

D'Silva, S., & Choudhuri, A. R. 1993, A&A, 272, 621
Galloway, D. J., & Jones, C. A. 1995, PASA, 12, 180
Galloway, D. J., & Moore, D. R. 1979, Geophys. Astrophys. Fluid Dynamics, 12, 73
Galloway, D. J., Proctor, M. R. E., & Weiss, N. O. 1977, Nature, 266, 686
Galloway, D. J., Proctor, M. R. E., & Weiss, N. O. 1978, J. Fluid Mech., 87, 243
Jones, C. A., & Galloway, D. J. 1993, J. Fluid Mech., 253, 297
Leka, K. D., Canfield, R. C., McClymont, A. N., & Van Driel Gesztelyi, L. 1996, ApJ, 462, 547
Longcope, D. W., Fisher, G. H., & Pevtsov, A. A. 1998, ApJ, 507, 117L
Longcope, D. W., Linton, M. G., Pevtsov, A. A., Fisher, G. H., & Klapper, I. 1999, in Magnetic Helicity in Space and Laboratory Plasmas, eds M. Brown, R. Canfield, & A. Pevtsov (http://solar.physics.montana.edu/dana/pubs.html)
Melrose, D. B. 1995, ApJ, 451, 391
Melrose, D. B. 1996, ApJ, 471, 497
Melrose, D. B. 1997, ApJ, 486, 521
Miyagoshi, T., Uchida, Y., Yabiku, T., Hirose, S., & Cable, S. 2001, PASJ, 53, 341

Parker, E. N. 1996, ApJ, 471, 497
Pevtsov, A. A., Canfield, R. C., & Metcalf, T. R. 1994, ApJ, 425, L117
Priest, E. R. 1982, Solar Magnetohydrodynamics (Dordrecht: D. Reidel)
Priest, E. R., & Forbes, T. G. 2000, Magnetic Reconnection (Cambridge: Cambridge University Press)
Proctor, M. R. E., & Galloway, D. J. 1979, J. Fluid. Mech., 91, 273
Schmidt, H. U. 1964, NASA Symposium on Solar Flares, NASA SP-50, ed. W. Hess, p. 107
Uchida, Y., & Shibata, K. 1988, Solar Phys., 116, 291
Uchida, Y., Miyagoshi, T., Yabiku, T., Cable, S., & Hirose, S. 2001, PASJ, 53, 311
Wheatland, M. S., & Uchida, Y. 1999, Solar Phys., 189, 163